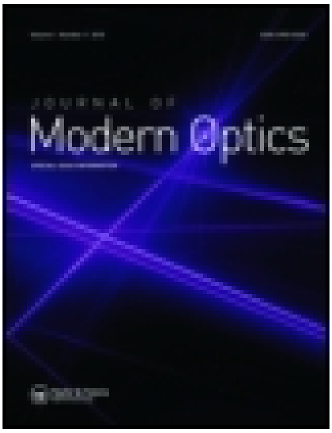

Optica Acta: International Journal of Optics
Publication details, including instructions for authors and subscription information:
http://www.tandfonline.com/loi/tmop19

A General Modal Theory for Reflection Gratings

J.R. Andrewartha [a] , G.H. Derrick [b] & R.C. McPhedran [b]
[a] Department of Physics, University of Tasmania, G.P.O. Box 252C, Hobart, Tasmania, Australia 7001
[b] Department of Theoretical Physics, University of Sydney, Sydney, New South Wales, Australia 2006
Published online: 14 Nov 2010.

OPTICA ACTA, 1981, VOL. 28, NO. 11, 1501–1516

A general modal theory for reflection gratings

J. R. ANDREWARTHA
Department of Physics, University of Tasmania,
G.P.O. Box 252C, Hobart, Tasmania, Australia 7001

G. H. DERRICK and R. C. McPHEDRAN
Department of Theoretical Physics, University of Sydney,
Sydney, New South Wales, Australia 2006

(*Received 1 April 1981*)

Abstract. The problem of diffraction from lossless reflection gratings is treated with a modal expansion formulation which incorporates an impedance condition on the mode eigenfunctions along the groove aperture. The theory for both fundamental polarizations is applied to three different grating profiles and is found to yield results which conform well with predictions of an established integral theory over a restricted range of groove depths. The upper bounds on these depths are approximately 0·2 periods for the symmetrical triangular profile and 0·5 periods for the semi-circular and sinusoidal profiles. Beyond these limits numerical instabilities occur and the results often fail to satisfy standard numerical tests.

1. Introduction

During the period since the introduction of high-speed computers, rigorous theories have been developed to account successfully for the diffraction from singly-periodic, plane gratings with grooves of virtually any profile. Hence, there is no need for new formalisms if it is desired only to make numerical calculations, with, for example, the aim of profile parameter optimization. However, it is worthwhile to develop additional theories if by so doing we can improve our general understanding of the spectral behaviour of gratings.

The currently available theories are based predominantly on integral [1–4] and differential methods [5, 6], in which the mechanism of the diffraction process for gratings with differing groove shapes is lost in a complexity of mathematics. In the integral method, the field above the grating is expressed in terms of an unknown function which, in treatments similar to that of Pavageau and Bousquet [2], is related to the induced current density on the surface. By satisfying the boundary condition, a Fredholm integral equation is derived from which a solution to the unknown function may be obtained. From this it is possible to reconstruct the plane-wave amplitudes. In the differential method, a solution is sought for a function in one variable which satisfies a system of ordinary coupled differential equations. In some cases, such systems have resulted from conformal transformation techniques in which the profile is mapped onto a coordinate axis at the expense of complicating the Helmholtz equation.

Analytic methods, in which the appropriate field quantity is everywhere describable by known expansions, are less complex than the above and provide an enhanced explanation of the action of particular gratings. To date, this type of

0030-3909/81/2811 1501 $02·00 © 1981 Taylor & Francis Ltd

method has only been rigorously applied to specific grating profiles. These are the rectangular (lamellar) profile [7–9], the triangular profile [10] and the semi-circular profile [11]. In [9], a modal method for the relatively simple lamellar grating has been exploited extensively to explain the resonance behaviour of that grating in terms of complex poles in the mode amplitudes.

A recent paper by Fox [12], on the general application of the modal method, verifies the validity of this kind of treatment in which the field in the groove region is expanded over a complete set of eigenfunctions and then matched to the diffracted field, represented by a plane-wave Rayleigh expansion. He shows that the scattering matrix in such a problem is unitary and satisfies the condition of reciprocity.

It is the aim of this paper to report on investigations of a modal expansion technique to solve the diffraction problem for a perfectly conducting reflection grating with grooves of arbitrary cross-section. Following its successful application to a semi-circular profile grating, an eigenvalue condition is employed, in which the eigenvalue is a real impedance analogous to the quantity D_{mm} used by Fox in [12].

Section 2 deals with the theoretical formulation of the scalar-wave problem for the fundamental cases of P and S polarizations, while §3 is concerned with the numerical implementation and describes some of the difficulties which were encountered, particularly in the case of deep grooves. In the domain where convergence is satisfactory, efficiencies in the diffracted orders have been calculated and compared with those provided by an integral formulation. This comparison is illustrated for the sinusoidal and the semi-circular profile for a Littrow mounting in the order -1 and also for a symmetrical triangular grating in a normal incidence mounting.

In the final section, possible reasons are discussed for the instability of the formalism, evident either when the groove depth-to-period ratio becomes sufficiently large or when an excessive number of modal terms is included in the calculations.

2. The formalism

2.1. *Notation and theoretical outline*

The periodic function $y=f(x)=f(x+d)$, for all x, is chosen to represent the surface separating free-space ($y>f(x)$) from the perfectly-conducting grating material ($y\leqslant f(x)$). This function is taken to lie in the lower-half xy plane, as shown in figure 1, and is assumed to equal zero on the intervals given by ($ld+c \leqslant x \leqslant (l+1)d$; $l=0, \pm 1, \pm 2, \ldots$). These intervals are referred to as the 'land' between the grooves. The aperture width c has a maximum value equal to d, while h is the overall groove depth.

The scalar-wave problem for P polarization is examined first in detail, with a summary of the treatment for S polarization being given in § 2.4.

Initially, then, an incident plane-wave is considered having its electric vector along the OZ axis, and its wave-vector $\mathbf{k}$ lying in the xy plane and at an angle θ to the y-direction. The plane waves scattered outwards from the grating also have their electric fields aligned with the OZ axis. Thus the problem is characterized entirely by the z-component of the electric field, which is a function of x and y only. Using an expansion of the type proposed by Rayleigh [13], and omitting the

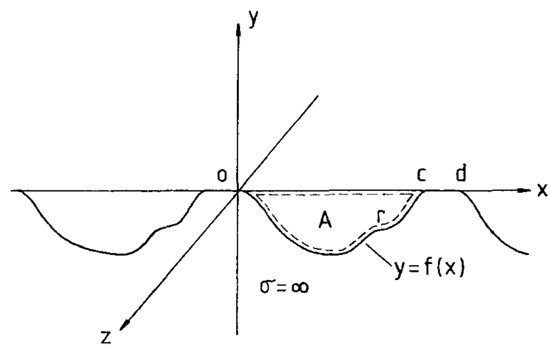

Figure 1. Geometry for the perfectly conducting reflection grating with arbitrary groove profile.

temporal dependent term $\exp(-i\omega t)$, the total electric field in the free-space region $y \geqslant 0$ is represented by

$$E^R(x, y) = \exp[i(\alpha_0 x - \chi_0 y)] + \sum_{n=-\infty}^{\infty} A_n \exp[i(\alpha_n x + \chi_n y)], \tag{1}$$

where λ is the wavelength,

and

$$\left.\begin{aligned} k &= |\mathbf{k}| = \frac{2\pi}{\lambda} \quad \text{is the wavenumber,} \\ \alpha_n &= k \sin\theta_n = k\left(\sin\theta + \frac{n\lambda}{d}\right) \\ \chi_n &= (k^2 - \alpha_n^2)^{1/2}, \quad \sin\theta_n \leqslant 1 \quad (\text{real orders: } n \in R) \\ &= i(\alpha_n^2 - k^2)^{1/2}, \quad \sin\theta_n > 1 \quad (\text{evanescent orders}). \end{aligned}\right\} \tag{2}$$

The first term in (1) corresponds to the incident wave of unit amplitude while the coefficients A_n are the amplitudes of the diffracted wave-field. In terms of these coefficients, energy propagating in the y-direction is conserved according to the relation

$$\sum_{n \in R} \left(|A_n|^2 \frac{\chi_n}{\chi_0} \right) = 1, \tag{3}$$

where each term in the expansion on the left represents the efficiency in the nth real order and is designated by $E(n)$.

Within the groove region A, the field is expanded in terms of a series of discrete eigenfunctions (modes) $u_m(x, y)$:

$$E^M(x, y) = \sum_{m=1}^{\infty} a_m u_m(x, y), \qquad 0 \leqslant x \leqslant c, \quad f(x) \leqslant y \leqslant 0, \tag{4}$$

where the a_m are the complex mode amplitudes. Each modal function u_m is chosen to be real-valued [12] and to satisfy the wave-equation

$$\left[\frac{\partial^2}{\partial x^2} + \frac{\partial^2}{\partial y^2} + k^2\right] u(x, y) = 0. \tag{5}$$

The relevant boundary conditions must also be satisfied. To this end the tangential component of the electric field should vanish on the perfectly-conducting grating surface, i.e.

$$u(x, f(x))=0, \qquad 0 \leqslant x \leqslant c. \tag{6}$$

A third condition must also be imposed to determine uniquely the mode functions. The proposed constraint has been successfully used in specifying the modal field in the groove region for the semi-circular profile grating [11]. This takes the form of an impedance condition which is applied to the field along the groove aperture:

$$\frac{\partial u(x, y)}{\partial y}=\beta u(x, y) \quad \text{for} \quad y=0,\ 0 \leqslant x \leqslant c. \tag{7}$$

β is an eigenvalue which must be real.

2.2. *The eigenvalue problem*

2.2.1. *Specification of the modal field*

A set of real-valued functions $\psi_p(x, y)$, which is similar to the set of eigenfunctions for the lamellar grating [7–9], is defined by the relation

$$\psi_p(x, y)=\sin\left(\frac{p\pi x}{c}\right)\frac{\sin(\mu_p y)}{\mu_p}, \qquad p=1, 2, 3, \ldots, \tag{8}$$

where

$$\mu_p^2=k^2-\frac{p^2\pi^2}{c^2} \tag{9}$$

and μ_p is chosen to be positive real or positive imaginary. ψ_p is a solution of the wave-equation and is seen to vanish along $y=0$, while $\partial\psi_p/\partial y$ forms an orthogonal set for $y=0$ on the interval $0 \leqslant x \leqslant c$.

A set of functions $\phi_p(x, y)$ is now defined by

$$\phi_p(x, y)=\frac{\partial\psi_p(x, y)}{\partial y}+\beta\psi_p(x, y). \tag{10}$$

By linearity, ϕ_p is a solution of the Helmholtz equation, and satisfies the condition given by (7). The functions $\phi_p(x, y)$ form an orthogonal set on $y=0$ for $0 \leqslant x \leqslant c$. The mode functions are now expanded in terms of the ϕ_p,

$$u(x, y)=\sum_{p=1}^{\infty} g_p\phi_p(x, y). \tag{11}$$

Substitution of (10) and (8) into this expression followed by application of the boundary condition given by (6), in a manner described below, leads to an infinite eigenvalue equation of the type

$$(G+\beta H)\mathbf{g}=0, \tag{12}$$

where G and H are real, square matrices, β is the eigenvalue of (7), and $\mathbf{g}$ is the corresponding eigenvector.

Following the appropriate truncation of G and H to finite dimension, the eigenvectors and eigenvalues may be evaluated by numerical means. Labelling the mth such solution for these quantities as $\mathbf{g}_m$ and β_m respectively and then expanding (11), one derives for the mth eigenmode in the groove region

$$u_m(x, y) = \sum_{p=1}^{\infty} g_{mp} \sin\left(\frac{p\pi x}{c}\right)\left[\cos(\mu_p y) + \beta_m \frac{\sin(\mu_p y)}{\mu_p}\right]. \tag{13}$$

2.2.2. *The mode boundary problem*

It is necessary to determine the g_{mp} and β_m such that the boundary condition given by equation (6) is satisfied. Inserting (13) in (6) yields

$$\sum_{p=1}^{\infty} g_{mp} \sin\left(\frac{p\pi x}{c}\right)\left[\cos(\mu_p f(x)) + \beta_m \frac{\sin(\mu_p f(x))}{\mu_p}\right] = 0, \qquad 0 \leqslant x \leqslant c. \tag{14}$$

The solution of this eigenvalue equation has been attempted by two different techniques—a point-matching method (P.M.M.) and a Fourier series method (F.S.M.). Both of these treatments have been used in the past by various authors (Petit [14], Jiracek [15]) in solving the diffraction problem using the now discredited Rayleigh approximation.

(1) *Point-matching method.* This technique simply involves sampling the profile at a discrete number of points, $((x_q, f(x_q), q = 1, 2, 3, \ldots)$ over a single period. Equation (14) is then in the form of (12) where the matrix elements G_{qp} and H_{qp} in that equation are given by

$$\left.\begin{aligned} G_{qp} &= \sin\left(\frac{p\pi x_q}{c}\right)\cos(\mu_p f(x_q)), \\ H_{qp} &= \sin\left(\frac{p\pi x_q}{c}\right)\frac{\sin(\mu_p f(x_q))}{\mu_p}. \end{aligned}\right\} \tag{15}$$

Once a suitable points distribution has been ascertained for the profile concerned, (15) can be simply implemented on the computer to find the β_m and g_{mp}.

(2) *Fourier series method.* This method consists of replacing the function given in the left-hand side of equation (14) by a Fourier series and then equating each Fourier coefficient to zero. The functions u_m vanish at $x = 0$, c and therefore may be expanded in terms of the complete set of functions $\sin(q\pi x/c)$:

$$u_m(x, f(x)) = \sum_{q=1}^{\infty} c_q \sin\left(\frac{q\pi x}{c}\right). \tag{16}$$

Equating the Fourier coefficients c_q to zero for $q = 1, 2, \ldots$ gives an equation again in the form of (12), where the matrix elements G_{qp} and H_{qp} are:

$$\left.\begin{aligned} G_{qp} &= \frac{1}{c}\int_0^c \cos(\mu_p f(x)) \sin\left(\frac{p\pi x}{c}\right)\sin\left(\frac{q\pi x}{c}\right) dx, \\ H_{qp} &= \frac{1}{c}\int_0^c \frac{\sin(\mu_p f(x))}{\mu_p} \sin\left(\frac{p\pi x}{c}\right)\sin\left(\frac{q\pi x}{c}\right) dx. \end{aligned}\right\} \tag{17}$$

(Note that in the case where $f(x)$ is an even function of x about $c/2$, only those matrix elements with $(p+q)$ even are non-zero.) Truncation of the Fourier series to a finite number of terms allows the eigenvalues and eigenvectors to be evaluated as with the previous method.

At this stage it is noted that the matrix $H^{-1}G$, whose eigenvalues $(-\beta)$ are sought via (12), is asymmetric. For the untruncated matrix, all the eigenvalues must be real, but no such guarantee exists when the matrix is truncated. This was also the case when the constraint prescribed by (7) was used to solve the eigenvalue problem for the semi-circular profile. However, it is interesting to note that a far greater proportion of the eigensolutions is found to be real when the formalism presented here is applied to that particular profile.

As was the case with the other theory, and for reasons of orthogonality demonstrated in the following section, only the real eigensolutions are chosen from the total of possible real and complex solutions. This procedure results in the rejection of only a small fraction of the eigensolutions.

2.2.3. *Orthogonality properties of the modes*

Consider the groove region A which is enclosed by the contour denoted Γ (figure 1). Application of Green's theorem to this region gives

$$\int_{\Gamma}\left(\frac{\partial u_l}{\partial \hat{n}}\overline{u_m}-\frac{\partial \overline{u_m}}{\partial \hat{n}}u_l\right)ds=\int_{A}(\overline{u_m}\,\nabla^2 u_l-u_l\,\nabla^2\overline{u_m})\,da,$$

where $u_m=u_m(x, y)$, $\hat{n}$ is a unit normal vector, ds is an element of arc length and da of area. Simplification of this expression with the aid of the wave-equation and the boundary condition (6) leads to

$$\int_0^c\left(\frac{\partial u_l}{\partial y}\overline{u_m}-\frac{\partial \overline{u_m}}{\partial y}u_l\right)_{y=0}dx=0.$$

Using (7), this reduces to

$$(\beta_l-\overline{\beta_m})\int_0^c(u_l\overline{u_m})_{y=0}\,dx=0. \tag{18}$$

With $l=m$, (18) implies that β_l must be real. There is then no loss of generality in taking the corresponding eigenfunction u_l to be real. With $l\neq m$, (18) implies that modes corresponding to different eigenvalues are orthogonal on the interval $0\leqslant x\leqslant c$:

$$\int_0^c u_l(x, 0)u_m(x, 0)=0, \qquad l\neq m. \tag{19}$$

Substitution of the appropriate expansions from (13) into (19) now gives the relation

$$\frac{c}{2}\sum_p g_{mp}g_{lp}=0, \qquad m\neq l. \tag{20}$$

This serves as a useful check on the orthogonality of the eigenvectors obtained from the numerical computation.

2.3. *Field matching*

Having specified the electric field in the free-space region by (1), and in the groove region by (4) and (13), it is now possible to solve the diffraction problem by determining the amplitudes a_m and A_n. This is accomplished by matching the field and its y-derivative across the interface between the two regions.

Continuity of E along $y=0$ for $0 \leqslant x \leqslant d$ is expressed by

$$\begin{aligned} E^R(x, 0) &= E^M(x, 0), \qquad 0 \leqslant x \leqslant c, \\ &= 0, \qquad c \leqslant x \leqslant d. \end{aligned}$$

On expanding this equality, then multiplying both sides by $\exp(-i\alpha_n x)$, and integrating over a period, one obtains

$$\delta_{0.n} + A_n = \frac{1}{d} \sum_{m=1}^{\infty} a_m \sum_{p=1}^{\infty} g_{mp} I_{pn}, \tag{21}$$

where I_{pn} is the inner-product

$$I_{pn} = \int_0^c \sin\left(\frac{p\pi x}{c}\right) \exp(-i\alpha_n x)\, dx \tag{22}$$

and $\delta_{0,n}$ is the Kronecker delta.

The y-derivative of E is continuous only on the groove aperture:

$$\frac{\partial E^R(x, 0)}{\partial y} = \frac{\partial E^M(x, 0)}{\partial y}, \qquad 0 \leqslant x \leqslant c.$$

Projection of this relation onto the set of functions $\{\sin(q\pi x/c)\}$ gives

$$-i\chi_0 \overline{I_{q0}} + \sum_{n=-\infty}^{\infty} i\chi_n A_n \overline{I_{qn}} = \frac{c}{2} \sum_{m=1}^{\infty} a_m \beta_m g_{mq}. \tag{23}$$

Inserting (22) into (23) and so eliminating A_n, one derives the following infinite linear system of equations in the a_m:

$$\sum_{m=1}^{\infty} a_m W_{mq} = 2i\chi_0 \overline{I_{q0}}, \tag{24}$$

where

$$W_{mq} = \sum_{n=-\infty}^{\infty} \left[\frac{i\chi_n \overline{I_{qn}}}{d} \left(\sum_{p=1}^{\infty} g_{mp} I_{pn}\right)\right] - \frac{c\beta_m g_{mq}}{2}. \tag{25}$$

Using available standard methods, (24) is solved numerically for the a_m, after which the diffracted wave amplitudes are evaluated from (21). The efficiencies in the propagating orders may then be computed from (3).

2.4. *S polarization*

In this case, the only non-zero component $H(x, y)$ of the magnetic field is aligned parallel to the generating axis of the grating. $H(x, y)$ is then the single unknown function. The treatment is very similar to that for P polarization and so the description here is confined to a summary of the essential differences between the two cases.

For this problem the wave-equation is unaltered and so with the exception of (6) (the boundary condition), (1)–(7) remain unchanged if $E(x, y)$ is replaced by $H(x, y)$. The unknown plane wave and modal coefficients will be denoted B_n and b_m respectively, in place of A_n and a_m. The appropriate boundary condition, implied by the continuity of the tangential component of **E**, is that the normal derivative of **H** be continuous. The relation analogous to (6) is therefore

$$n_x \frac{\partial u(x, f(x))}{\partial x} + n_y \frac{\partial u(x, f(x))}{\partial y} = 0, \qquad 0 \leqslant x \leqslant c, \tag{26}$$

where $\mathbf{n} = (n_x, n_y, 0)$ is the unit normal vector to the grating profile:

$$\left.\begin{aligned} n_x &= \frac{-f'(x)}{\sqrt{1+[f'(x)]^2}}, \\ n_y &= \frac{1}{\sqrt{1+[f'(x)]^2}}. \end{aligned}\right\} \tag{27}$$

The function from which the modes are to be generated is now defined as

$$\psi_p(x, y) = \cos\left(\frac{p\pi x}{c}\right) \frac{\sin(\mu_p y)}{\mu_p}, \qquad p = 0, 1, 2, \ldots, \tag{28}$$

from which the expression equivalent to (13) for the eigenmodes is

$$u_m(x, y) = \sum_{p=0}^{\infty} g_{mp} \cos\left(\frac{p\pi x}{c}\right)\left[\cos(\mu_p y) + \beta_m \frac{\sin(\mu_p y)}{\mu_p}\right] \tag{29}$$

It is noted that the $p = 0$ term is now included in the expansion.

In satisfying the boundary problem, produced by substituting equation (29) into equation (26), an eigenvalue equation, (12), is formed, wherein the matrix elements for the P.M.M., corresponding to (15) for the P polarization case, are given by:

$$\left.\begin{aligned} G_{qp} &= -\mu_p n_{y,q} \cos\left(\frac{p\pi x_q}{c}\right) \sin(\mu_p y_q) - \frac{p\pi}{c} n_{x,q} \sin\left(\frac{p\pi x_q}{c}\right) \cos(\mu_p y_q), \\ H_{q,p} &= n_{y,q} \cos\left(\frac{p\pi x_q}{c}\right) \cos(\mu_p y_q) - \frac{p\pi}{c} n_{x,q} \sin\left(\frac{p\pi x_q}{c}\right) \frac{\sin(\mu_p y_q)}{\mu_p}. \end{aligned}\right\} \tag{30}$$

Here $n_{x,q}$, $n_{y,q}$ are obtained if x is replaced by x_q in (27).

For the F.S.M., a similar treatment to that for the previous polarization is valid, but with a Fourier cosine series being the appropriate representation. The matrix elements G_{qp} and H_{qp} are derived to be

$$\left.\begin{aligned} G_{qp} &= \frac{1}{c} \int_0^c \left[-\frac{p\pi}{c} n_x \sin\left(\frac{p\pi x}{c}\right) \cos(\mu_p f(x)) \right. \\ &\qquad \left. - \mu_p n_y \cos\left(\frac{p\pi x}{c}\right) \sin(\mu_p f(x)) \right] \cos\left(\frac{q\pi x}{c}\right) dx, \\ H_{qp} &= \frac{1}{c} \int_0^c \left[-\frac{p\pi}{c} n_x \sin\left(\frac{p\pi x}{c}\right) \frac{\sin(\mu_p f(x))}{\mu_p} \right. \\ &\qquad \left. + n_y \cos\left(\frac{p\pi x}{c}\right) \cos(\mu_p f(x)) \right] \cos\left(\frac{q\pi x}{c}\right) dx. \end{aligned}\right\} \tag{31}$$

Again, if $f(x)$ is an even function of x about $c/2$, only those matrix elements with $(p+q)$ even are non-zero.

The field matching along $y=0$ for S polarization proceeds as before but with H being continuous only for $0 \leqslant x \leqslant c$, and $\partial H/\partial y$ being continuous across the interface from $x=0$ to $x=d$. Satisfying these requirements, one obtains the two equations

$$\overline{J_{q0}} + \sum_{n=-\infty}^{\infty} B_n \overline{J_{qn}} = c\varepsilon_q \sum_{m=1}^{\infty} b_m g_{mq} \tag{32}$$

and

$$-\delta_{0,n} + B_n = \frac{1}{i\chi_n d} \sum_{m=1}^{\infty} b_m \beta_m \left(\sum_{p=0}^{\infty} g_{mp} J_{pn} \right), \tag{33}$$

where

$$J_{pn} = \int_0^c \cos\left(\frac{p\pi x}{c}\right) \exp(-i\alpha_n x)\, dx \tag{34}$$

and

$$\varepsilon_p(x) = \tfrac{1}{2}, \qquad p \geqslant 1,$$
$$= 1, \qquad p = 0.$$

The final linear system to be solved for the unknown modal amplitudes b_m is obtained by inserting (33) into (32):

$$\sum_{m=1}^{\infty} b_m Z_{mq} = 2\overline{J_{q0}}, \tag{35}$$

where

$$Z_{mq} = \beta_m \sum_{n=-\infty}^{\infty} \left[\frac{i\overline{J_{qn}}}{d\chi_n} \left(\sum_{p=0}^{\infty} g_{mp} J_{pn} \right) \right] + c\varepsilon_q g_{mq} \tag{36}$$

This system is solved numerically using the same method as before—the plane wave amplitudes B_n being recovered from (33) and efficiency values from (3).

3. Application of the theory

Extensive work carried out on the numerical application of the theory presented in the previous section has produced many fruitful results, but unfortunately has also unearthed limitations which detract from its potential usefulness. This section deals with various aspects of the numerical implementation and includes a discussion of the problems encountered and the attempts made to overcome them. Also given are some efficiency curves which compare the predictions of this formalism with those of two alternative theories.

3.1. *Numerical considerations*

The initial step in solving the problem numerically is the evaluation of the integrals contained in (22) and (34) and, in the case of the F.S.M., those in equations (17) and (31). The inner-products expressed by the former two equations are dealt with straightforwardly since they are easily converted to a simple analytic form. The integrals in the latter two equations are, however, not reduced simply for profiles not composed of linear facets, and must be computed numerically. The routine employed for this purpose used adaptive Romberg extrapolation and it was found that great care had to be exercised, especially for deep grooves where the integrand is not particularly well behaved.

The next step involves truncation of the infinite series to appropriate finite limits. Two independent truncations are necessary—one indirectly determining the number of modes to be considered and the other directly specifying the number of diffracted-wave terms. If the formalism is to prove valid, then the calculated solutions for the amplitudes (a_m, b_m) and (A_n, B_n) should converge towards their true values as the truncation limits are extended. Ideally, the accepted limit occurs when successive values lie within a desired tolerance and comply with numerical checks, such as those of energy conservation, reciprocity [16] and phase properties [17]. For many of the situations tested, compliance with these criteria was unfortunately not always satisfactory due to numerical instabilities. Results of some of these tests are given.

The infinite series in (1) was truncated at $p = \pm Q$. No numerical difficulties were encountered in determining a suitable value for this limit and a value of $Q = 8$ was found to be ample when only 2 or 3 orders are propagating. This gives a total of 17 orders being taken into consideration.

With respect to the F.S.M., for symmetric profiles it can be seen for P polarization from (17) that the matrix elements G_{qp} and H_{qp} are non-zero for $(p+q)$ odd and are zero for $(p+q)$ even, where $p, q = 1, 2, 3, \ldots$ Hence, the eigenvectors may be divided into two sets—'even modes' with g_{mp} equal to zero for even p, and 'odd modes' with g_{mp} equal to zero for odd p. It is easily shown that these modes correspond respectively to the symmetry relations:

$$u_m\left(\frac{c}{2}+x, y\right) = u_m\left(\frac{c}{2}-x, y\right),$$

$$u_m\left(\frac{c}{2}+x, y\right) = -u_m\left(\frac{c}{2}-x, y\right).$$

For S polarization, the eigenvectors with elements g_{mp} equal to zero for $p = 1, 3, 5, \ldots$ relate to even modes, while those with zero elements for $p = 0, 2, 4, \ldots$ correspond to odd modes. This intrinsic structure of G and H for symmetric profiles permits decoupling of the eigenvalue problem (12) into two eigenvalue problems—one for even modes and one for odd modes. This means that on reconstruction of the eigenvectors, the alternate elements are precisely zero. It also allows for a saving of computer time (due to the halving of matrix dimensions) while the values for the determinants are also improved.

As regards the P.M.M., if the points distribution is chosen to be symmetrical about the centre of the groove, then this symmetry is contained in G and H so that the eigenvectors, after computation, should have alternate elements equal to zero. In practice, it has been found that numerical errors can emerge at this point, and so in this respect the F.S.M. is superior.

For asymmetric profiles, the properties of evenness and oddness of modes do not apply.

Consider now the truncation limits of the modal series. If the P.M.M. is used, then the limit on the number of modal terms is governed by the number of profile points chosen, while if the F.S.M. is selected then the limit is the number of Fourier coefficients chosen in (16). Denoting either limit as M, then the square matrices G and H of (12) are of dimension M, making this the maximum possible number of real eigensolutions. As previously mentioned, $H^{-1}G$ is not a symmetrical matrix and when it is truncated both real and complex solutions are possible. Furthermore, there is no guarantee that the eigenvectors form a complete set. In the results obtained so far, however, especially with the F.S.M., most of the eigenvalues are real. Occasionally, with the P.M.M. and for large values of M, say greater than 16, a complex-conjugate pair of eigenvalues is produced. These may be discarded in an attempt to form a solution with the remainder of the real eigenvalues. Such a procedure is sometimes successful, but may lead to intolerable errors, especially if it results in an imbalance in the number of even and odd modes. Unlike the determination of a satisfactory value for Q, numerical difficulties are often met in optimizing the parameter M. Again these difficulties become more evident for large groove depths, where high values for M can cause the formation of complex eigenvalues, or can make the matrices G and H badly conditioned. For $M=12$ to 16, however, quite reasonable results are achieved for some profiles, up to a normalized groove depth of $h/d=0{\cdot}5$, when only a few orders are propagating. For shallower grooves, as few as eight modes are sufficient. Some of the numerical problems can often be overcome by choosing the better method of the F.S.M. and the P.M.M., by altering the points distribution of the latter or be redefining ψ_p to be $\psi_p/\cos(\mu_p h)$. The F.S.M. method is found to be the more successful in the majority of cases. It enables computations to be carried out for deeper grooves and permits a higher value for M before numerical instabilities appear. It does, however, carry the added complexity of numerical integration. One exception to the superiority of the F.S.M. occurs in the case of the semi-circular profile grating, for which numerical tests are more accurately satisfied for the P.M.M. Note that only minor differences between the results have been detected for the various points distributions when this method has been used for that grating.

The other two profiles studied intensively are the sinusoidal and symmetrical triangular profiles. Using the F.S.M. reasonable results are obtained for these gratings in the -1 Littrow and normal incidence mountings, for normalized groove depths up to $0{\cdot}4$ for the former grating and $0{\cdot}2$ for the latter.

3.2. *Numerical tests on the formalism*

One obvious check on the formalism is to consider the rectangular-groove grating. For such a profile the eigenvalues β_m are known analytically—being $\mu_m \cot(\mu_m h)$ for P polarization and $-\mu_m \tan(\mu_m h)$ for S polarization, where h is the groove depth.

Using the P.M.M., this profile was sampled at points $(x_q, -h)$, $q=1, 2, \ldots$ where $0<x_q<c$. The eigenvalues, eigenvectors and plane-wave amplitudes computed using this method were in excellent agreement with those furnished by a modal method specifically designed for the rectangular-groove grating [9].

A second test compared a set of odd and even mode eigenvalues obtained for the semi-circular groove grating, with those calculated by an alternative modal theory [11], based on the same eigenvalue condition (7). Table 1 displays this comparison for a grating with a normalized groove radius of $c/2d=0{\cdot}4$ where the wavelength is $\lambda/d=1{\cdot}4$ and the grating is operated in the -1 Littrow mount. These results are in good agreement. It is interesting to observe that for higher

Table 1. Comparison of eigenvalues with those provided by an alternative modal theory designed specifically for the semi-circular groove profile. The parameters used for this grating in a Littrow mounting are $c/d=0{\cdot}8$, $h/d=0{\cdot}4$, $\lambda/d=1{\cdot}4$, $\theta=44{\cdot}427^\circ$ while calculations were made with $Q=8$ and $M=12$.

P polarization		*S* polarization	
General modal theory	Semi-circular profile theory	General modal theory	Semi-circular profile theory
2·38‡	2·39	−104·90‡	−100·39
6·85†	6·89	0·23†	0·23
11·02‡	11·09	6·28‡	6·07
15·10†	15·18	10·89†	10·73
19·13‡	19·25	15·06‡	14·91
23·13†	23·29	19·12†	19·02
27·12‡	22·90	23·13‡	21·46
31·09†	26·46	27·12†	25·17

† Odd modes.
‡ Even modes.

orders, the *S* and *P* polarization eigenvalues become equal at a value very close to $m\pi/c$ which is the common value reached by the eigenvalues of the rectangular-groove profile for large m.

The method has been found to provide very rewarding results for the sinusoidal profile. For $c/d=1{\cdot}0$ and depths up to $h/d=0{\cdot}4$, the calculations satisfied adequately numerical checks while also agreeing well with predictions of an integral theory [2, 18] in situations where only a few orders propagate. Table 2 shows the variation in efficiency with increasing M for one wavelength with this profile. It is unusual that the *S* polarization efficiencies converge faster and are more accurate than those for *P* polarization when they are compared with the integral theory results. Table 3 demonstrates the accuracy with which a reciprocity test was satisfied. Figure 2 displays efficiency curves computed using ten modes

Table 2. Efficiency and phase of the zero order, and also energy defect, as a function of the number of modes characterizing the groove field. A sinusoidal grating of $h/d=0{\cdot}4$ was considered with normally incident radiation of wavelength $\lambda/d=0{\cdot}9$. The number of plane-wave terms used was 17.

	P polarization			*S* polarization		
M	$E(0)$	Phase(0)	Energy defect (per cent)	$E(0)$	Phase(0)	Energy defect (per cent)
8	0·3180	−7·7	2·505	0·5405	−20·45	0·121
10	0·3157	−6·72	0·896	0·5434	−20·46	−0·198
12	0·3146	−6·26	0·487	0·5416	−20·45	0·003
14	0·3150	−5·96	0·248	0·5415	−20·44	0·005
16	0·3154	−5·77	0·127	0·5415	−20·44	0·000
18	0·3159	−5·66	0·039	0·5416	−20·44	0·001
Integral theory	0·3172	−4·65	0·000	0·5415	−20·58	0·010

Table 3. Reciprocity results illustrating efficiency, phase and total diffracted energy (T.D.E.), for a sinusoidal grating of groove depth $h/d=0{\cdot}4$ and irradiated at a wavelength of $\lambda/d=0{\cdot}8$. Computations were carried out with 14 modes and 17 plane-wave terms. In Problem 1, $\theta=0°$, while in Problem 2 the -1 order was returned at an angle of incidence given by $\theta=53{\cdot}1301°$.

		P polarization			*S* polarization		
	Order *n*	$E(n)$	Phase(n)	T.D.E.	$E(n)$	Phase(n)	T.D.E.
Problem 1	0	0·1628	52·17	0·9985	0·7451	5·95	1·0001
	±1	0·4179	−148·72	—	0·1275	−121·49	—
Problem 2	−1	0·4194	−148·72	1·0008	0·1274	−121·49	1·0000

for a grating in a -1 Littrow configuration and having a normalized groove depth of 0·4. It also contains a comparison of predictions of the F.S.M. and P.M.M. methods with those of the integral theory. It can be seen that excellent agreement is achieved with the F.S.M., with the maximum discrepancy being only 10 per cent in the wavelength interval where only two real orders exist. This occurs near a resonance anomaly.

As previously mentioned, and in contrast to the above, it is the P.M.M. rather than the F.S.M. which has provided results which are in better agreement with those of alternative theories for the semi-circular groove grating. In figure 3 these comparisons are exhibited for the -1 Littrow mount and a normalized groove radius of 0·4. The excellent agreement seen here for ten profile points is maintained for this profile for groove radii up to the maximum of 0·5 periods.

Acceptable results have been achieved for the symmetrical triangular profile but only using the F.S.M. Figure 4 demonstrates the closeness of efficiencies calculated using this method (with 12 modes) to those of the integral theory for a normal incidence mounting. The small discrepancy seen in the spectra for *S* polarization at wavelengths below $\lambda/d=0{\cdot}6$ coincides with the poor energy conservation of the modal formalism for shorter wavelengths. With normalized

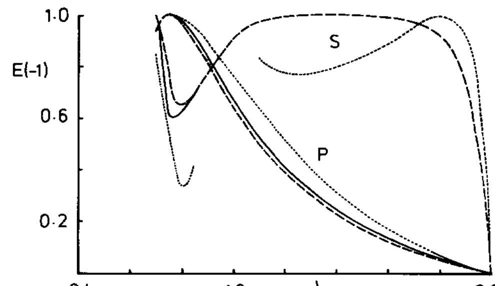

Figure 2. Efficiency curves for a sinusoidal profile grating of normalized groove depth 0·4 and operated in a -1 Littrow mounting. Solid line: integral theory; dotted line: modal theory P.M.M.; dashed line: modal theory F.S.M. Ten modes were employed for the latter two cases.

groove depths above the value of 0·2 used for these curves, energy defects were found to worsen to the extent that calculations for this profile become grossly inaccurate.

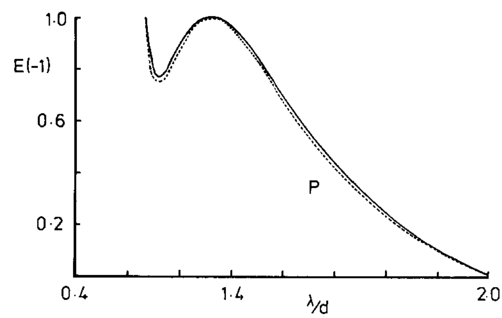

(*a*)

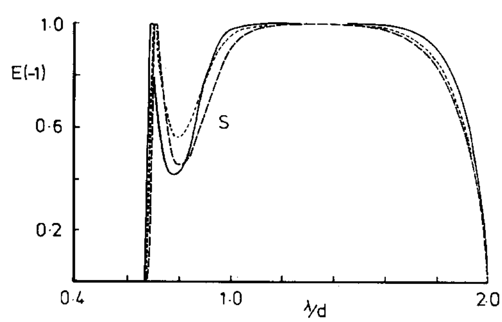

(*b*)

Figure 3. −1 Littrow efficiency curves for a semicircular groove grating of normalized groove depth 0·4. (*a*) *P* polarization; (*b*) *S* polarization. Solid line: integral theory; dotted line: modal theory P.M.M.; dashed lined: modal theory F.S.M. Results obtained with an alternative modal theory [11] coincide too closely to the dotted line to be included.

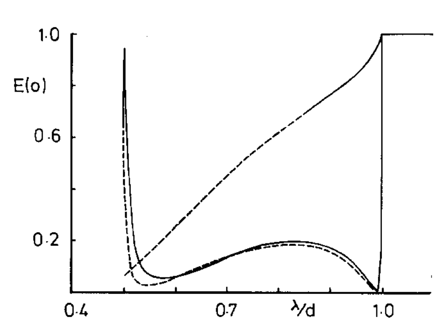

Figure 4. Efficiency curves for a symmetrical triangular groove profile of normalized depth 0·2 and operated in a normal incidence mounting. Solid line: integral theory; dotted line: modal theory F.S.M. (12 modes).

4. Discussion of the method

It is evident from findings discussed in the previous section that instabilities prevent extensive application of this method in its present form to general profile gratings with arbitrarily deep grooves. A brief discussion is given here to outline the reasons which we believe to lie behind this failing. Although many of the problems are numerical, the underlying faults are most probably due to the mode eigenfunctions not forming a complete set over the groove region as a consequence of the eigenvalue problem not being framed in terms of symmetric matrices.

Consider again the eigenvalue equation (12). We have shown in § 2.2.3 that, if the matrices G and H are not truncated, then all eigenvalues β are real, and all eigenvectors $\mathbf{g}$ corresponding to different eigenvalues are orthogonal over the interval $0<x<d$, $y=0$. However, when G and H are truncated as above, the boundary conditions on $y=f(x)$ are only approximately satisfied. Some complex eigenvalues then occur, and (especially for deeper grooves) eigenvectors fail to be (even approximately) orthogonal. We have adopted the somewhat arbitrary procedure of discarding the complex eigenvalues and corresponding eigenvectors, and have thereby obtained a numerical procedure with (in some cases) inadequate convergence.

To overcome this defect, it would be sufficient to reformulate the eigenvalue problem in such a way as to lead to an expression of the form of (12), but with $(H^{-1}G)$ a real, symmetric matrix.

5. Conclusion

We have described investigations concerning the application of a modal expansion technique to the scalar-wave diffraction problem for reflection gratings of infinite conductivity and with arbitrary groove profile. The formalism is based on an impedance constraint which is applied at the interface separating the groove region from the free-space region above the grating. This constraint requires that on that interval the value of each eigenfunction specifying the field in the groove region be proportional to its normal derivative. The constant of proportionality is an eigenvalue. The modes are subsequently constructed from waveguide functions similar to those appropriate to a lamellar grating.

The theory for the two fundamental polarizations has been tested numerically and efficiencies have been computed for three different profiles and compared with those predicted by an integral formalism. The profiles considered were those of the sinusoidal, semi-circular and symmetrical triangular gratings. Satisfactory agreement in efficiency was achieved but only for moderate groove depths—these ranging up to half a period for the first two profiles mentioned and to a fifth of a period for the third. Eigenvalues produced by this method for a semi-circular profile grating were found to conform well with those provided by an alternative modal treatment dependent on the same impedance constraint.

Numerical problems were encountered in the implementation of the formalism whenever groove depths greater than those listed above were tried or whenever a large number of modes was included to characterize the groove field. These problems have been attributed to the fact that the prescribed eigenvalue constraint does not lead to an eigenvalue problem for symmetric matrices.

Future work in this area should be directed towards the development of a formulation, which, if based on an eigenvalue technique, must necessarily generate real and orthogonal solutions for the modes.

Le problème de la diffraction par des réseaux par réflexion sans pertes est traité au moyen d'une formulation de développement modal qui comprend une condition d'impédance sur les fonctions propres modales le long de l'ouverture gravée. La théorie pour les deux polarisations fondamentales est appliquée à trois différents profils de réseau et on trouve qu'elle conduit à des résultats en bon accord avec les prévisions d'une théorie établie pour un domaine limité de profondeurs de traits. Les limites supérieures pour ces profondeurs sont approximativement 0,2 période pour le profil triangulaire symétrique et 0,5 période pour les profils semi-circulaire et sinusoidal. Au delà de ces limites, des instabilités numériques se produisent et les résultats manquent souvent de satisfaire les tests numériques standards.

Diese Arbeit behandelt das Problem der Beugung an verlustfreien Reflexionsgittern mit einer modalen Entwicklung, welche eine Impedanzbedingung für die Moduseigenfunktionen entlang der Furchenöffnungen enthält. Diese Theorie wird für beide fundamentalen Polarisationen auf drei verschiedene Gitterprofile angewandt und ergibt Resultate, welche über einen beschränkten Bereich von Furchentiefen gut mit den Vorhersagen einer etablierten Integraltheorie übereinstimmen. Die obere Grenze für die Furchentiefen liegt bei etwa 0,2 Perioden für das symmetrische Dreiecksprofil und bei 0,5 Perioden für halbkreis- und sinusförmige Profile. Jenseits dieser Grenzen treten numerische Instabilitäten auf und die Ergebnisse genügen oft nicht numerischen Standardtests.

References

[1] Petit, R., and Cadilhac, M., 1967, *C. r. hebd. Séanc. Acad. Sci. Paris*, **264**, 1441.
[2] Pavageau, J., and Bousquet, J., 1970, *Optica Acta*, **17**, 469.
[3] Van den Berg, P. M., 1971, Thesis, Delft.
[4] Kalhor, H., and Neureuther, A., 1971, *J. opt. Soc. Am.*, **61**, 43.
[5] Nevière, M., Cerutti-Maori, G., and Cadilhac, M., 1971, *Optics Commun.*, **3**, 48.
[6] Nevière, M., Cadilhac, M., and Petit, R., 1973, *I.E.E.E. Trans. Antennas Propag.*, **21**, 37.
[7] Maystre, D., and Petit, R., 1972, *Optics Commun.*, **5**, 90.
[8] Wirgin, A., and Deleuil, R., 1969, *J. opt. Soc. Am.*, **59**, 1348.
[9] Andrewartha, J. R., Fox, J. R., and Wilson, I. J., 1979, *Optica Acta*, **26**, 69.
[10] Jovicevic, S., and Sesnic, S., 1972, *J. opt. Soc. Am.*, **62**, 865.
[11] Andrewartha, J. R., Derrick, G. H., and McPhedran, R. C., 1981, *Optica Acta*, **28**, 1177.
[12] Fox, J. R., 1980, *Optica Acta*, **27**, 289.
[13] Rayleigh, Lord, 1907, *Proc. R. Soc.* A, **79**, 399.
[14] Petit, R., 1963, *Revue Optique*, **42**, 263.
[15] Jiracek, G. R., 1973, *I.E.E.E. Trans. Antennas Propag.*, **21**, 393.
[16] Petit, R., 1967, *Optica Acta*, **14**, 301.
[17] Botten, L. C., 1978, Thesis, University of Tasmania, Australia.
[18] McPhedran, R. C., 1973, Thesis, University of Tasmania, Australia.